

11. HIGH-RESOLUTION ROCK-MAGNETIC STUDY OF CEARA RISE SEDIMENTS AT SITE 925¹

Peter A. Solheid,² Subir K. Banerjee,² Carl Richter,³ and Jean-Pierre Valet⁴

ABSTRACT

A variety of rock-magnetic measurements was made on sediment samples from Ceara Rise, Leg 154, Site 925 of the Ocean Drilling Program. Ceara Rise sediments are composed of marine carbonates and terrigenous material from the Amazon Fan. Bulk susceptibility, which measures approximately the concentration of strongly magnetic particles (e.g., magnetite, maghemite) in the sediment, can be used as a climate proxy signal that is based on the dilution of terrigenous material by ocean-derived carbonates. During interglacial periods, the high-susceptibility terrigenous material is diluted, resulting in a minimum in susceptibility. This hypothesis is supported by the inverse correlation between the smoothed susceptibility record and the $\delta^{18}\text{O}$ low latitude record. Anhyseretic remanent magnetization (ARM), contributed primarily by magnetic grains from 0.1 to 15 μm , was normalized by susceptibility (χ), giving a parameter that is sensitive to magnetic grain size. Variations of ARM/ χ show high values during interglacials and low values during glacials. The source of this material is most likely from an increase of Amazon Basin soil runoff during interglacial periods.

INTRODUCTION

Ceara Rise (5°N 44° W) is located just north of the equator, approximately 700 km from the mouth of the Amazon River (Fig. 1) where it intersects the Atlantic Ocean's deep water flow paths (Curry, Shackleton, Richter, et al., 1995). The sediment is composed of marine carbonates and terrigenous material delivered from the Amazon Basin. The sediment covers the entire Cenozoic in age and ranges in thickness from 950 to 1300 m. Five sites were cored during Leg 154 of the Ocean Drilling Program (ODP) to complete a bathymetric transect from Site 925 at a depth of 3040 m to Site 929 at a depth of 4355 m. The sediments for our study came from Site 925, which is the shallowest of the five sites and located well above the Carbonate Compensation Depth (CCD) (Curry, Shackleton, Richter, et al., 1995).

The sediments consist mainly of clay, calcareous nannofossils, and foraminifers in varying amounts. The top 30 m consist of grayish brown nannofossil clay with foraminifers alternating with light brownish gray clayey nannofossil ooze with foraminifers. Below this interval, from 30 to 135 mbsf, the sediments consist of nannofossil ooze with varying amounts of foraminifers and steadily increasing clay towards the top of the subunit (Curry, Shackleton, Richter, et al., 1995). A composite section was constructed by splicing together sections of different cores by matching overlapping magnetic susceptibility and color data to create a continuous sedimentary section (Hagelberg et al., 1992). The composite section for Site 925 consists of cores from Holes 925A, 925B, and 925C resulting in a continuous sediment record measured in meters composite depth (mcd) for most of the upper 300 m from the middle Miocene to the late Pleistocene (Curry, Shackleton, Richter, et al., 1995).

A multi-parameter rock-magnetic study was conducted on these sediments to seek a high-resolution rock-magnetic proxy signal of climate cycles, possibly both at Milankovitch and sub-Milankovitch in scale. Various rock-magnetic measurements were made in order to

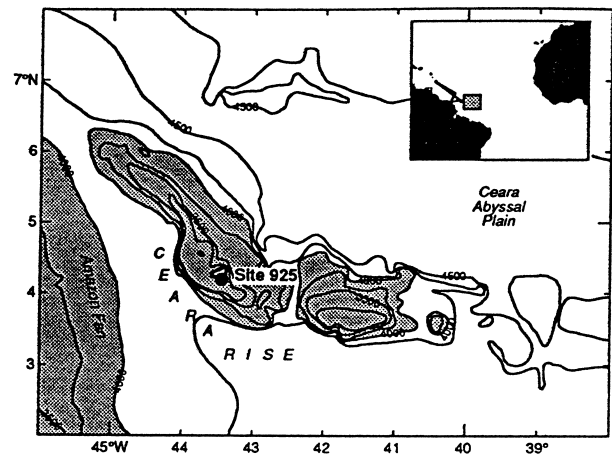


Figure 1. Location map of Ceara Rise showing Site 925 (Mountain and Curry, 1995).

determine concentration, grain size, and composition of the magnetic grains for the top 6 mcd of the composite section. Based on nannofossil dates determined on board, the sedimentation rate is approximately 40 mcd/m.y. (Curry, Shackleton, Richter, et al., 1995). At 6 mcd, the age of the sediment should be 150 k.y.

SAMPLING AND EXPERIMENTAL METHOD

Low-field magnetic susceptibility (χ_{lf}) and anhyseretic remanent magnetization (ARM) were measured at room temperature (300 K). Hysteresis parameters were measured next at room temperature for selected samples. For selected samples, low-field magnetic susceptibility and saturation isothermal remanent magnetization (SIRM) were measured as a function of temperature, both lower and higher than 300 K.

Room Temperature Measurements

Samples were selected from Sections 154-925C-1H-1 through 1H-4 to provide a high resolution record of deposition encompassing $\delta^{18}\text{O}$

¹Shackleton, N.J., Curry, W.B., Richter, C., and Bralower, T.J. (Eds.), 1997. *Proc. ODP, Sci. Results*, 154: College Station, TX (Ocean Drilling Program).

²Institute for Rock Magnetism, University of Minnesota, Minneapolis MN 55455-0128, U.S.A. peat@tc.umn.edu.

³Ocean Drilling Program, 1000 Discovery Drive, Texas A&M University, College Station, TX 77845-4857, U.S.A.

⁴Institut de Physique du Globe, 4 Place Jussieu, 75252 Paris Cedex 05, France.

Stages 1–6. A total of 214 samples were taken in unoriented 2.5 cm³ sample tubes at 2- to 5-cm intervals and then transferred for magnetic measurements into standard spectroscopy cuvettes cut to 1 cm³ cubes. Measurements were made in order of increasing magnetic field intensity so that previous measurements would not affect later measurements. Low-field magnetic mass susceptibility χ_{lf} was measured for each sample in a Kappabridge model KLY-2 susceptibility bridge (Geofyzika Brno) with an inducing field of 3.8×10^{-4} T. Low field susceptibility is contributed by the ferrimagnetic, antiferromagnetic, paramagnetic, and diamagnetic components of the sample. The measurements were corrected for the susceptibility of the empty cube (-9.21×10^{-8} m³/kg) and normalized to mass. Repeated measurements show the error from this source to be less than 0.5%. The samples were then given an ARM in a modified Schonsted demagnetizer, by applying a small (50×10^{-6} T) DC biasing field superimposed on a decaying alternating field with a peak value of 100 mT. The samples were then measured on a 2G Enterprises 3-axis cryogenic magnetometer, and values were normalized to mass. The empty cubes have no measurable ARM greater than the error, estimated to be 1% from repeated measurements. Following this, hysteresis loops were measured on selected samples on a vibrating sample magnetometer (VSM) and normalized to mass. From the hysteresis measurements we obtained parameters related to magnetic mineralogy and grain size: saturation magnetization (σ_s), which is the magnetization at 0.75 T (corrected for the linear response of dia-, para-, and antiferromagnetic constituents). High-field susceptibility (χ_{hf}) was determined by calculating the slope of the closed high-field (0.6–0.75 T) portion of the loop. χ_{hf} is a measurement of the antiferromagnetic, diamagnetic, and paramagnetic content of the sample.

Temperature Dependent Measurements

We selected 10 samples to examine the magnetic mineralogy with low temperature SIRM. Approximately 0.15 g of material is cooled down to 20 K and exposed to a 2.5 T magnetic field for 20 seconds. At this temperature even the finest grains are thermally stable and can acquire a remanence. The sample is then gradually warmed to room temperature while the SIRM is measured in zero field at 5 K intervals. From these measurements, certain magnetic minerals can be identified by characteristic spin transitions at which a loss of remanence occurs at a characteristic temperature. Susceptibility vs. temperature was also measured on approximately 0.15 g of sample from room temperature to 700°C on a furnace-equipped, Kappabridge model KLY-2 susceptibility bridge modified with flowing Argon gas. Upon heating, at the Curie point the thermal energy overcomes the magnetic ordering of the ferri- and antiferromagnetic content, the weak magnetic field is no longer able to induce a magnetization in the sample, and susceptibility is reduced to zero. Ferri- and antiferromagnetic minerals can be identified by this method.

RESULTS

Magnetic Susceptibility

Low-field magnetic susceptibility shows variations with wavelengths in the order of 20 to 100 cm (Fig. 2). The values range from 4×10^{-8} to 1.6×10^{-7} m³/kg. The measurements agree well with the whole core susceptibility measurements made on board the *JOIDES Resolution*. The discrete samples provide a higher resolution and show smaller scale variations that cannot be detected with the pass-through equipment. Magnetic susceptibility is predominantly affected by the concentration of magnetic grains but can be affected by grain size as well. Measurements made on board ship show that susceptibility is negatively correlated to calcium carbonate and therefore predominately a carbonate concentration proxy (Curry, Shackleton, Richter, et al., 1995). Magnetic susceptibility correlates inversely with the low-latitude $\delta^{18}\text{O}$ stack (Bassinot et al., 1994) (Fig. 3). The agreement between the two

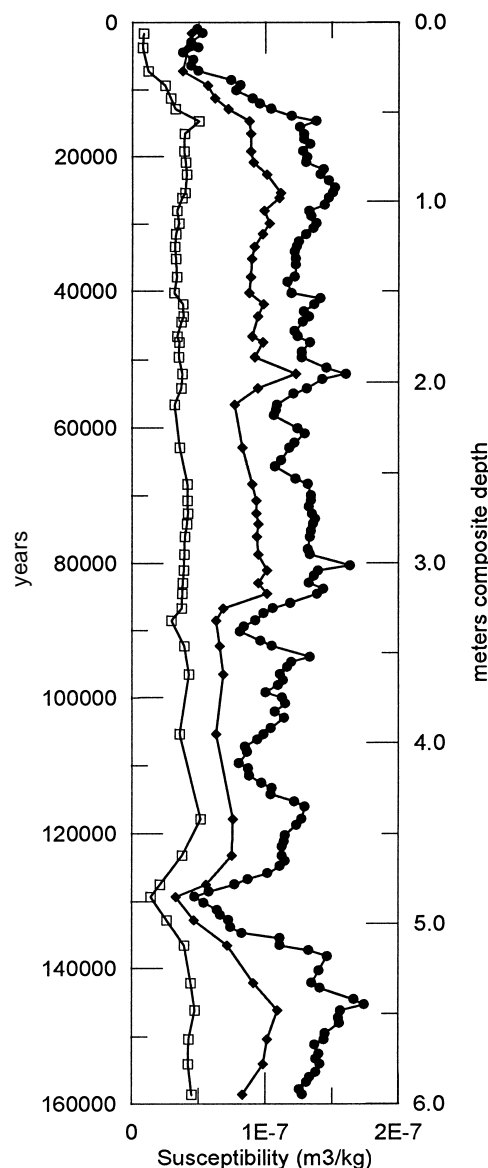


Figure 2. Low-field (solid circles) and high-field (open squares) susceptibility variations with depth. Note that all of the features of χ_{lf} remain after χ_{hf} is subtracted (solid diamonds). Left y-axis shows years.

data sets leads us to confirm the preliminary shipboard interpretation. Para- and diamagnetic susceptibility are contributed by clay, quartz, carbonates, and other non-iron-bearing minerals. χ_{hf} is contributed mainly by paramagnetic clay and diamagnetic minerals (calcium carbonate). High-field susceptibility (χ_{hf}) as described above is small in magnitude and varies from 1×10^{-8} to 6×10^{-8} m³/kg. By subtracting χ_{hf} from χ_{lf} we can obtain the contribution of the ferrimagnetic portion (or magnetite) of the sediment (Fig. 2). This calculation indicates that the variations in susceptibility are primarily due to the ferrimagnetic concentration.

Anhyseretic Remanence Magnetization

The ARM varied from $4.5\text{E}-5$ to $9.5\text{E}-5$ Am²/kg indicating a change in the concentration of fine single-domain (SD) to pseudo-single-domain (PSD) magnetite and other ferrimagnetic minerals. Measurements of ARM show a positive correlation with susceptibil-

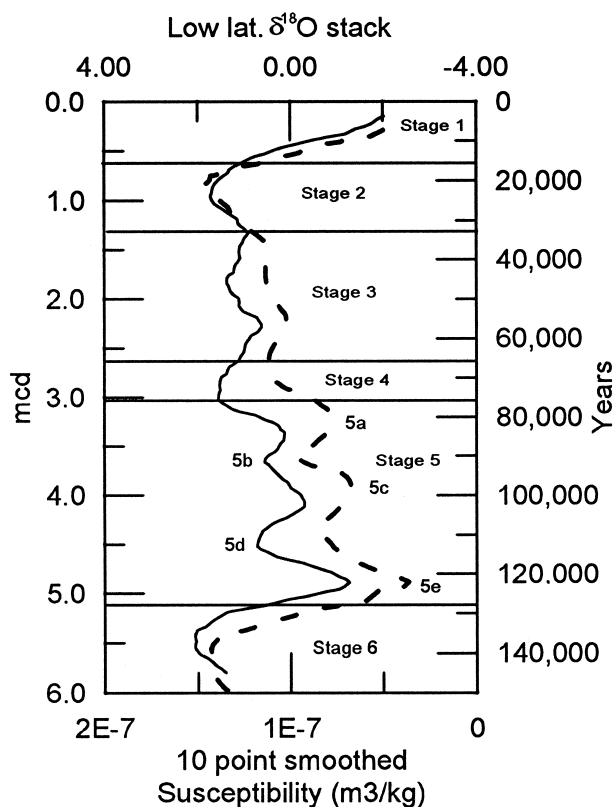


Figure 3. Comparison of 10-point smoothed susceptibility (solid line) and the low-latitude $\delta^{18}\text{O}$ stack of Bassinot et al., 1994 (dashed line). The high degree of correlation implies that variations in susceptibility are induced by climate change.

ity from 1 to 3 mcd (Fig. 4). Above and below this region the correlation breaks down and even appears to become negatively correlated below 3 mcd.

Hysteresis Parameters

Hysteresis parameters are shown in Figure 5. The saturation magnetization (σ_s) varies from 0.3×10^2 to 9×10^2 Am²/kg and saturation remanence (σ_{rs}) varies from 0.5×10^{-3} to 2.2×10^{-3} Am²/kg. Coercivity (H_c) ranges from 12.5 to 18 mT and coercivity of remanence (H_{cr}) ranges from 35 to 50 mT. All magnetic minerals contribute to σ_s while σ_{rs} is sensitive only to the concentration of SD and multidomain (MD) ferromagnetic particles. H_c and H_{cr} are dependent on both mineralogy and grain size. There is a sharp drop in H_c and H_{cr} (3.5 and 13 mT respectively) at about 1 mcd; below this depth H_c and H_{cr} remain fairly constant. A comparison of the ratios σ_{rs}/σ_s to H_{cr}/H_c yields information about the domain state and hence the grain size of the magnetic particles (Day et al., 1977; Dunlop, 1986). The average value of σ_{rs}/σ_s is 0.22 and the average value of H_{cr}/H_c is 2.6. Figure 6 shows the data clustered in the center of the PSD region on a plot of the hysteresis ratios (Day et al., 1977).

Temperature Dependent Results

Susceptibility vs. temperature measurements show a strong peak between 250° and 300° C that is twice the amplitude of the baseline. A second peak occurs between 450° and 550° C just prior to the Curie point where the susceptibility drops to zero. Figure 7 shows two characteristic χ_{lf} vs. temperature curves from samples from above and be-

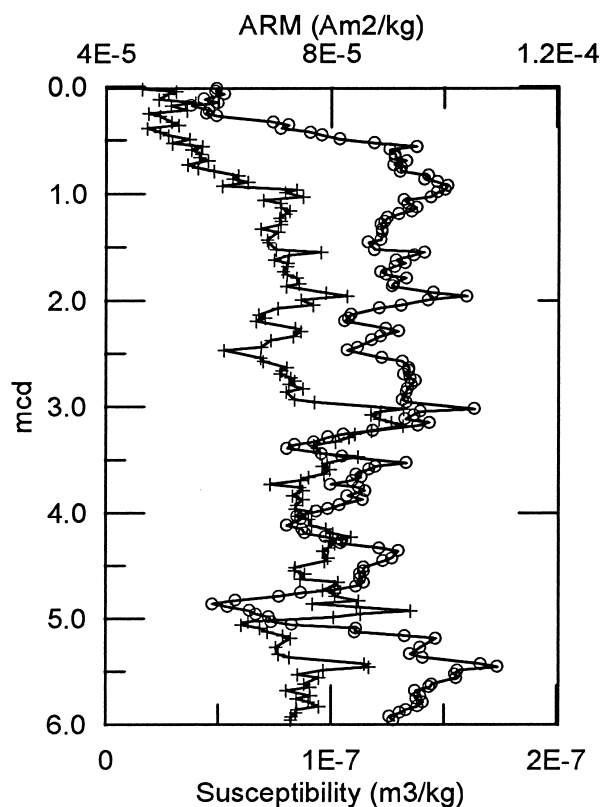


Figure 4. Downcore variations of susceptibility (open circles) and anhysteretic remanent magnetization (+). Between 1 and 4 mcd the susceptibility and ARM are correlated.

low the coercivity drop at 1 mcd. The peak between 250° and 300° C indicates the possible presence of pyrrhotite (Rochette et al., 1990) both above and below the coercivity drop. The loss of susceptibility near 580° C (the Curie point of magnetite) indicates that magnetite is the dominant magnetic mineral present in the samples. Low-temperature decay of saturation isothermal remanent magnetization in zero ambient field show high gradients of decrease of remanence between 20 and 60 K and gradual decay of remanence to 300 K following a step transition at 110 K. Figure 8 shows the decay of SIRM as a function of temperature and the derivative of the decay curve, which reveals small-scale variations in the amplitude and the position of transitions. The sharp decay of SIRM (acquired at 20 K) between 20 and 60 K indicates thermal unblocking in super paramagnetic (SP) ultra fine particles (<30 nm for magnetite), (Néel, 1949; Bean and Livingston, 1959; Cullity, 1972; Hunt et al., 1995). Larger grains of magnetite are indicated by the presence of the Verwey transition occurring at 118 K as indicated by the sharp gradient change of the curves.

DISCUSSION

Magnetic Mineralogy

Because of the low concentration of the magnetic phase (see below), it was not possible to identify the magnetic minerals by x-ray diffraction. Hysteresis loops show saturation at fields on the order of 0.2 T, as expected for magnetite or a mineral close to it in composition. Susceptibility vs. temperature curves show a major drop between 550° and 600° C, close to the Curie point (580° C) of pure magnetite. The susceptibility peak between 250° and 300° C is, however, close to 320° C, the susceptibility peak of pyrrhotite (Rochette et al.,

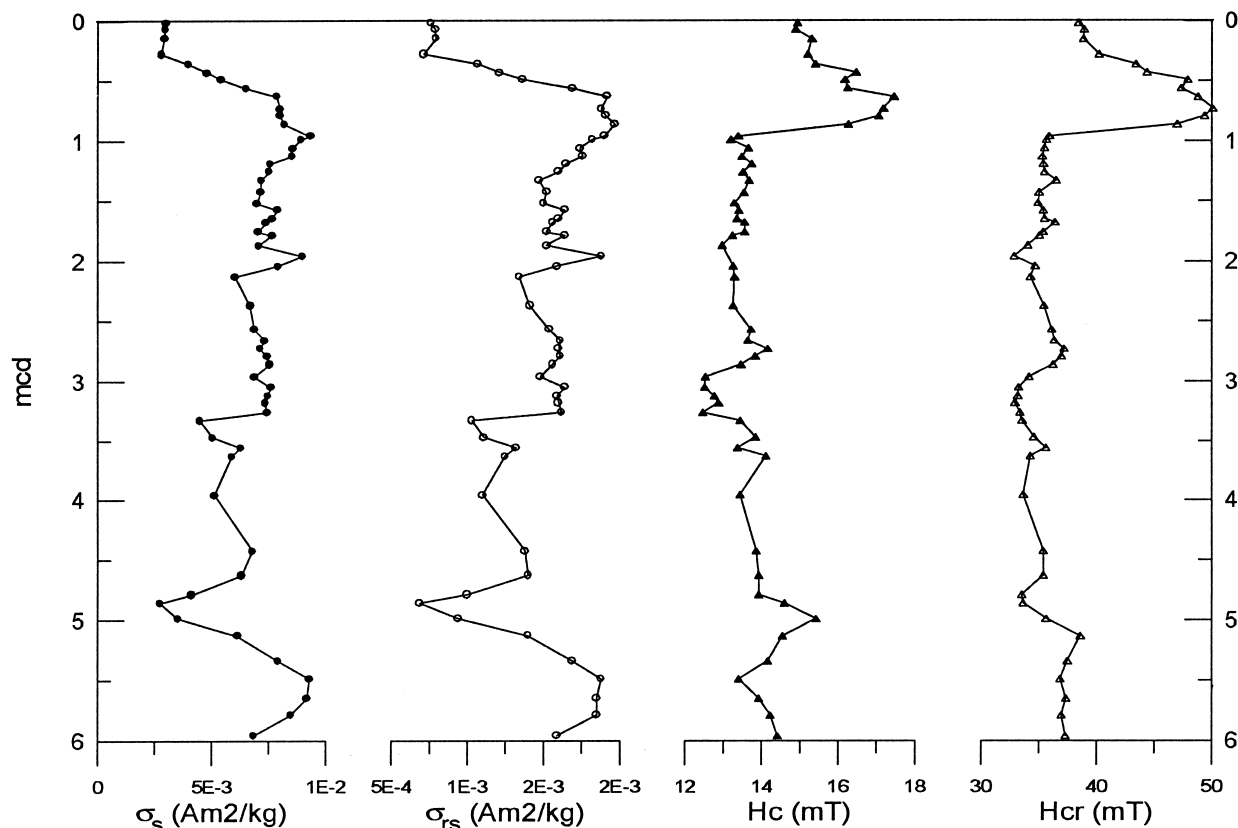


Figure 5. Hysteresis parameters vs. depth. Note the similarity between saturation magnetization (σ_s) (closed circles) and saturation remanence (σ_{rs}) (open circles), indicating that variations are due to single-domain and larger particles. Coercivity (H_c) (closed triangles) and coercivity remanence (H_{cr}) (open triangles) show a dramatic drop at near 1 mcd.

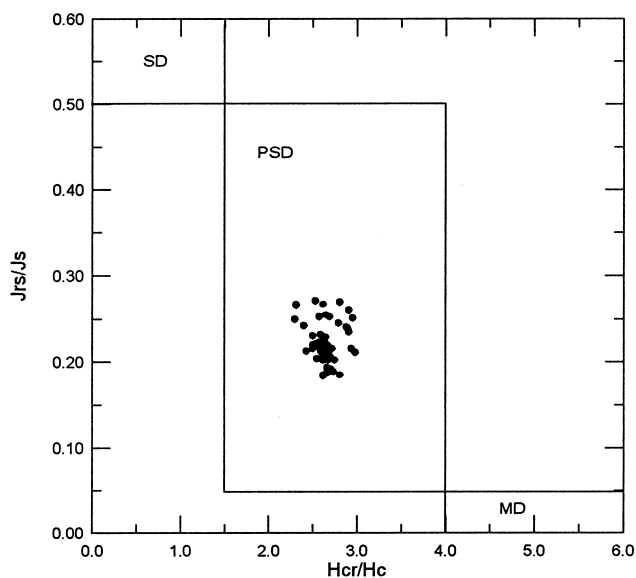


Figure 6. Plot of hysteresis parameter ratios (Day et al., 1977) show that all samples contain magnetite with a relatively uniform pseudo-single-domain grain size.

1990). The best evidence for magnetite comes from the ubiquitous observation of the characteristic Verwey transitions at 118K. Pending future experiments, it is reasonable to conclude that the main magnetic mineral is magnetite.

Magnetite Concentration

If magnetite is the chief magnetic mineral present, its concentration can be determined by dividing the observed saturation magnetization (σ_s) with that expected for pure magnetite, 92 Am²/kg. For most of the samples, i.e., below 0.6 m depth, average value of σ_s was 7.5×10^{-3} Am²/kg, leading to a magnetite concentration of ~0.0082%. This is very close to the mean value of 0.0072% observed by Richter et al. (this volume) for 114 samples from Site 929. In the top 0.6 m of our site, average σ_s decreases to $\sim 3.5 \times 10^{-3}$ Am²/kg, leading to a magnetite concentration of ~0.0038%. We suspect that this drop of nearly 54% is most likely caused by higher water content at the top.

Low-field magnetic susceptibility can be used as a proxy for magnetite concentration as long as grain size does not display a large variability, especially at the lower end (superparamagnetic, diameter <30 nm) of the size spectrum. As we will show below, the grain size of our samples is very uniform, falling within the middle of the PSD range, between 0.1 and 15 μ m. If dissolution were contributing to the loss of susceptibility we would see a loss of the finer grains, but, as we will show below, the proportion of finer grains increases when susceptibility is low. Therefore, the observed magnetic susceptibility variations about the mean can be interpreted as concentration variation of magnetite and CaCO₃ (Curry, Shackleton, Richter, et al., 1995). As we have further shown, the temporal record of susceptibil-

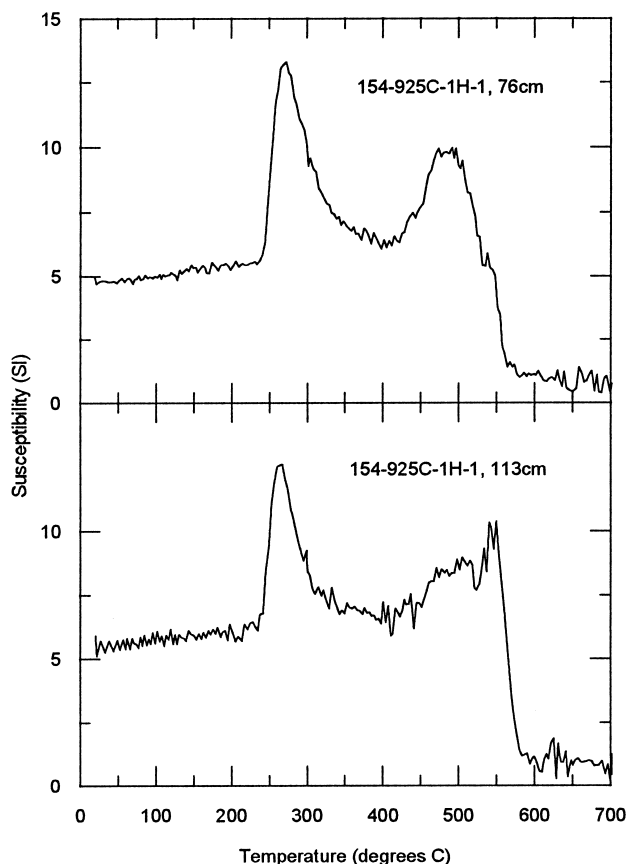


Figure 7. Susceptibility vs. temperature of two samples above (Sample 154-925C-1H-1, 76 cm) and below (Sample 154-925C-1H-1, 113 cm) the drop in coercivity and coercivity remanence at 1 mcd. Both samples show a peak near 300°C, the Curie point of pyrrhotite and a loss of susceptibility near 580°C, the Curie point of magnetite.

ity at Site 925 is inversely correlated with the low-latitude $\delta^{18}\text{O}$ stack (Bassinot et al., 1994).

Grain-Size Variation

Average grain-size information for magnetite can be obtained from a plot of the hysteresis parameters σ_{rs}/σ_s vs. H_{cr}/H_c (Day et al., 1977). Our data are well clustered in the middle of the PSD size-range, 0.1–15 μm (Fig. 6). A finer scale variation in grain size of magnetite can be obtained from the ratio of ARM/χ (Banerjee et al., 1981; King et al., 1982). A high value of the ratio signifies the presence of SD ($\sim 0.1 \mu\text{m}$) and small PSD ($\sim 1 \mu\text{m}$) grains. We find strong increases in ARM/χ during the Holocene and the previous interglacial (isotopic stage 5) (Fig. 9). Along with Richter et al. (this volume), we regard the source of the magnetite/maghemite as the terrigenous sediments composing the Amazon Fan, which is currently the main source of terrigenous material to the Ceara Rise. Therefore, high concentrations of SD and smaller PSD grains are likely from sediment input during interglacials when high rainfall and large surface run-off may have occurred in the Amazon drainage basin.

Diagenesis

The sharp drop in H_c and H_{cr} values at 0.95 mcd in the upper part of the sediment core is most likely a diagenetic effect caused by sulfate reduction (Leslie et al., 1990; Karlin, 1990). This dissolves SD

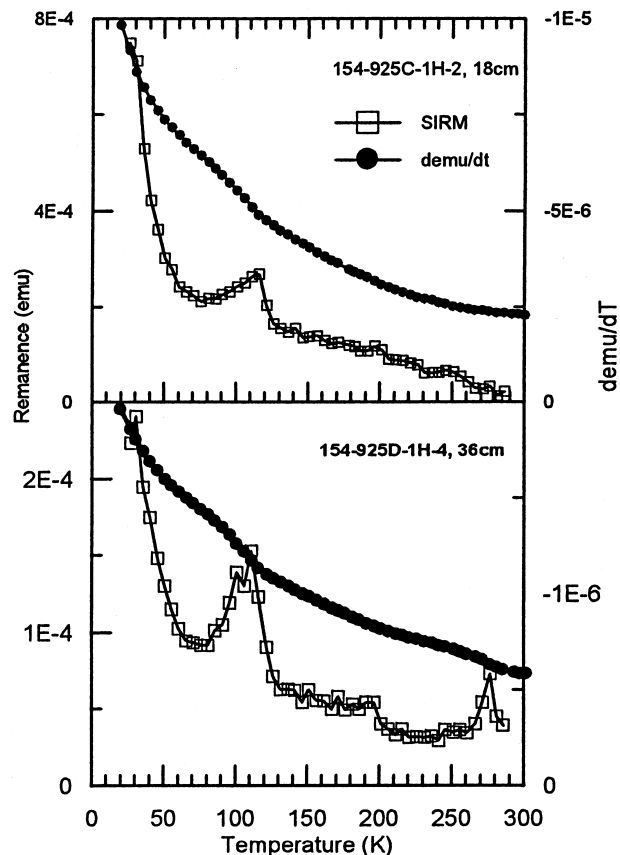


Figure 8. Thermal demagnetization of low temperature saturation isothermal remanent magnetization show that super paramagnetic grains as indicated by the sharp decrease in remanance between 20 and 60 K and larger grains of magnetite are present as noted by the Verwey transition at 118 K. The derivative of the demagnetization curve clearly shows smaller scale changes in both the magnitude and position of the transition.

magnetite grains with high H_c and H_{cr} values. The drop also corresponds to a change in color from reddish brown (0–0.95 mcd) to gray (0.95–6 mcd). Other magnetic parameters are not strongly affected by this drop indicating it may be due to the loss of a high-coercivity but weakly magnetic material such as hematite or goethite. This observation could explain why a corresponding decrease in σ_s does not exist. Furthermore, the heating experiments show a susceptibility peak at $\sim 275^\circ\text{C}$ both above and below the jump in H_c values at 0.95 mcd, which suggests the presence pyrrhotite. If sulfate reduction occurred below the H_c transition boundary, the pyrrhotite peak should not be present.

CONCLUSION

A high-resolution record of multiple magnetic proxies at Site 925 has been obtained for the last 150 k.y. Magnetic susceptibility, which is inversely correlated with temperature and CaCO_3 , shows oscillations that correspond to Milankovitch cycles. Magnetic measurements indicate that the main magnetic carrier is magnetite or maghemite but pyrrhotite may also be present. The concentration of magnetite varies from 0.0038% above 1 mcd to 0.0082% below 1 mcd. The average magnetic grain size ranges from 0.1–15 μm and is fairly uniform throughout the samples. High values of ARM/χ indicate increased fine-grained magnetite ($\sim 0.1 \mu\text{m}$) during interglacials.

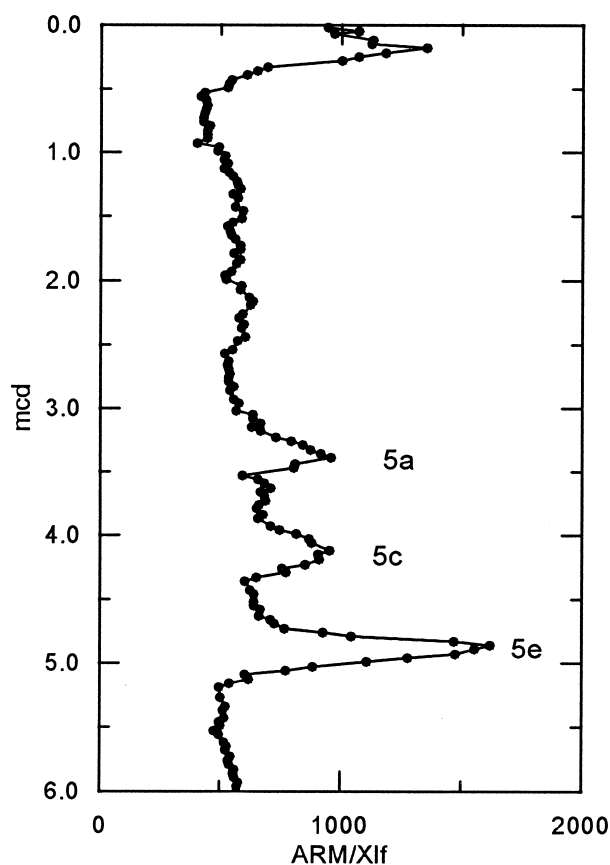


Figure 9. Anhyseretic remanence magnetization (ARM), a grain-size-dependent parameter, normalized to low-field susceptibility (to remove concentration variations), provides a measure for fine single-domain (SD) and small pseudo-single-domain (PSD) grain sizes. During interglacials (0–0.5 mcd and 3.2–5.2 mcd, see Fig. 3) the ratio is some 50%–100% higher than during glacials (0.5–3.2 mcd).

ACKNOWLEDGMENTS

We thank the crew and scientists aboard the *JOIDES Resolution* for their support and long days during this high-recovery leg. This paper is contribution No. 9603 of the Institute for Rock Magnetism which is funded by the Keck Foundation, NSF, and the University of Minnesota. We would also like to thank Bernie Housen for discussion leading to this manuscript and Mike Jackson for review, assistance, and discussion in preparing this manuscript.

REFERENCES

- Banerjee, S.K., King, J.W., and Marvin, J., 1981. A rapid method for magnetic granulometry with applications to environmental studies. *Geophys. Res. Lett.*, 8:333–336.
- Bassinot, F.C., Labeyrie, L.D., Vincent, E., Quidelleur, X., Shackleton, N.J., and Lancelot, Y., 1994. The astronomical theory of climate and the age of the Brunhes-Matuyama magnetic reversal. *Earth Planet. Sci. Lett.*, 126:91–108.
- Bean, C.P., and Livingston, J.D., 1959. Superparamagnetism. *J. Appl. Phys.*, 30:120S–129S.
- Cullity, B.D., 1972. *Introduction to Magnetic Materials*: Reading, MA (Addison-Wesley).
- Curry, W.B., Shackleton, N.J., Richter, C., et al., 1995. *Proc. ODP, Init. Repts.*, 154: College Station, TX (Ocean Drilling Program).
- Day, R., Fuller, M., and Schmidt, V.A., 1977. Hysteresis properties of titanomagnetites: grain-size and compositional dependence. *Phys. Earth Planet. Inter.*, 13:260–267.
- Dunlop, D.J., 1986. Hysteresis properties of magnetite and their dependence on particle size: a test of pseudo-single-domain remanence models. *J. Geophys. Res.*, 91:9569–9584.
- Hagelberg, T., Shackleton, N., Pisias, N., and Shipboard Scientific Party, 1992. Development of composite depth sections for Sites 844 through 854. In Mayer, L., Pisias, N., Janecek, T., et al., *Proc. ODP, Init. Repts.*, 138 (Pt. 1): College Station, TX (Ocean Drilling Program), 79–85.
- Hunt, C.P., Banerjee, S.K., Han, J.-M., Solheid, P.A., Oches, E.A., Sun, W.-W., and Liu, T.-S., 1995. Rock-magnetic proxies of climate change in the loess-paleosol sequences of the western Loess Plateau of China. *Geophys. J. Int.*, 123.
- Karlin, R., 1990. Magnetite diagenesis in marine sediments from the Oregon continental margin. *J. Geophys. Res.*, 95:4405–4419.
- King, J.W., Banerjee, S.K., Marvin, J., and Özdemir, Ö., 1982. A comparison of different magnetic methods for determining the relative grain size of magnetite in natural materials: some results from lake sediments. *Earth Planet. Sci. Lett.*, 59:404–419.
- Leslie, B.W., Lund S.P., and Hammond, D.E., 1990. Rock magnetic evidence for the dissolution and authigenic growth of magnetic minerals within anoxic marine sediments of the California continental borderland. *J. Geophys. Res.*, 95:4437–4452.
- Mountain, G.S., and Curry, W.B., 1995. Cruise Ew9209: Site survey for Leg 154. In Curry, W.B., Shackleton, N.J., Richter, C., et al., *Proc. ODP, Init. Repts.*, 154: College Station, TX (Ocean Drilling Program), 39–52.
- Néel, L., 1949. Théorie du traînage magnétique des ferromagnétiques en grains fins avec applications aux terres cuites. *Ann. Geophys.*, 5:99–136.
- Rochette, P., Fillion, G., Mattéi, J.-L., and Dekkers, M.J., 1990. Magnetic transition at 30–34 Kelvin in pyrrhotite: insight into a widespread occurrence of this mineral in rocks. *Earth Planet. Sci. Lett.*, 98:319–328.

Date of initial receipt: 12 December 1995

Date of acceptance: 26 August 1996

Ms 154SR-134